

Modeling mesoscale uncertainty for concrete in tension

Nathan Tregger[†]

Department of Civil and Environmental Engineering, McCormick School of Engineering and Applied Science, Northwestern University, 2145 Sheridan Road, Evanston, IL 60208-3109, USA

David Corr

*Exponent Failure Analysis Associates Inc., 185 Hansen Court,
Suite 100, Wood Dale, IL, 60191, USA*

Lori Graham-Brady

*Department of Civil Engineering, Whiting School of Engineering, Johns Hopkins University,
3400 North Charles Street, Baltimore, MD 21218-2608, USA*

Surendra Shah

Department of Civil and Environmental Engineering, McCormick School of Engineering and Applied Science, Northwestern University, 2145 Sheridan Road, Evanston, IL 60208-3109, USA

(Received July 25, 2006, Accepted September 1, 2007)

Abstract. Due to heterogeneities at all scales, concrete exhibits significant variability in mechanical behavior from sample to sample. An understanding of the fundamental mechanical performance of concrete must therefore be embedded in a stochastic framework. The current work attempts to address the connection between a two-dimensional concrete mesostructure and the random local material properties associated within that mesostructure. This work builds on previous work that has focused on the random configuration of concrete mesostructures. This was accomplished by developing an understanding of the effects of variations in the mortar strength and the mortar-aggregate interfacial strength in given deterministic mesostructural configurations. The results are assessed through direct tension tests that are validated by comparing experimental results of two different, pre-arranged mesostructures, with the intent of isolating the effect of local variations in strength. Agreement is shown both in mechanical property values as well as the qualitative nature of crack initiation and propagation.

Keywords: stochastic modeling; concrete; generalized method of cells; aggregate-mortar interface; fracture mechanics

1. Introduction

There are several sources of uncertainty that play a role in the performance of a structure. These sources include uncertainty in the loadings (e.g. earthquake and high winds), structural geometry

[†]Corresponding Author, E-mail: n.tregger@northwestern.edu

(due to design and construction errors) and in the capacity of the material. The ability to account for these uncertainties allows accurate implementation of safety factors and perhaps a reduction of a structure's life-cycle cost.

Uncertainty associated with the structural material is especially important for concrete structures. At the macroscale, concrete is treated as a homogeneous material, which is suitable for most design purposes. However, when considering the fracture processes of concrete, the analysis must focus on the finer mesoscale due to the localization of failure. At this mesoscale, interactions between mortar and aggregate dictate the initiation and progression of fracture, processes that dominate the failure behavior of concrete. Uncertainty at the mesoscale includes the random mechanical properties of the mortar, the aggregate, and the mortar-aggregate interface, as well as the randomness in size, shape and placement of coarse aggregates within the mortar.

Typically in the local mechanical analysis of concrete, uncertainty of material properties and cracking behavior are considered in a local averaging or crack band scheme as demonstrated by Bažant and Oh (1983), among others. The effects of material randomness have been historically incorporated into design codes in an inefficient manner, and it is necessary to pursue accurate models of this uncertainty to allow for efficient structural design as recommended by Bažant and Yu (2003).

One approach to addressing heterogeneous mesostructures is to perform a finite element analysis based on digital imagery. In this approach, each element of the finite element mesh corresponds to a pixel in a digitized image of the microstructure of interest. One of the most well-known examples of this is Object Oriented Finite element analysis (OOF), which is developed by National Institute of Standards and Technologies (NIST) and can be freely downloaded from their website (García, *et al.* 2002). The advantage to this approach is that it explicitly accounts for the shapes, sizes and distribution of aggregates. The disadvantage, however, is that the characterization of material randomness based on this technique would require digitized mesostructures from a large number of experimental specimens. This route is typically expensive and work-intensive. Furthermore, the potential exists for artificial stress concentrations to occur at sharp corners in the mesostructure, an effect that is more the result of the digitization and imaging process than of the true material structure (Graham-Brady, *et al.* 2003). Another approach is to numerically simulate the material mesostructure, taking advantage of inexpensive computational power as compared to preparing and imaging many physical specimens. The main problem with this method is that a significant amount of information is required in order to accurately represent in these simulations the aggregate sizes, shapes and placement (Bentz 2000, Grigoriu, *et al.* 2007, Graham-Brady and Xu 2006). In many cases this information (such as third-order correlation functions) is unavailable due to lack of data.

The current paper describes the application of a moving-window generalized method of cells (GMC) to the analysis of concrete with debonding. Moving-window GMC is a combination of the two approaches described above, which relates the mesostructure directly to the local mechanical behavior of the composite allowing subsequent computational simulation of mechanical properties to account for material uncertainty. In a sense, the approach can be viewed as a way to "smooth" the mesostructure, making analysis more computationally tractable. The moving-window GMC approach is computationally efficient, does not make any geometric assumptions and also has the ability to capture local features of the mesostructure. In a study by Corr and Graham (2003), this technique was applied to concrete in order to analyze the effects of spatial randomness in the concrete mesostructure; however, the parameters required at the interfaces were not well understood and no experimental benchmarks were available to confirm the results.

The current work combines experimental and computational work that is essentially in a two-dimensional environment. In reality, concrete is a particulate-based composite in which the third dimension is extremely important. While some experimental procedures do exist for analyzing material mesostructures in three-dimensions, they are limited in their application. For example, X-ray tomography combined with digital image correlation is an excellent candidate for studying local stress-strain behavior in a three-dimensional medium (Landis, *et al.* 2003); however, for fine resolutions this technique is generally limited to a sample size of approximately 1 cm^3 , making this approach impractical for materials like concrete where the mesostructure of interest is typically larger. For the computational models, the moving-window GMC technique has been applied to three-dimensional particulate composites in Baxter, *et al.* (2001). Due to the complexity of the three-dimensional experiments and the enormous quantity of data used in the associated computational models, this work focuses on two-dimensional models and experiments as a basis for verifying the efficacy of moving-window GMC relative to experimentally obtained results.

In this work, experiments are conducted to verify the moving-window GMC model for concrete both in terms of the mean and variation of mechanical properties as well as the nature of fracture formation and propagation. In order to isolate the effects of the random interfacial properties and mortar strength, deterministic mesostructures are used for the model and the experiments. A direct tensile test utilizing a closed-loop, displacement-control method is conducted to obtain stress-displacement curves so that mechanical properties can be extracted. The results are then compared to those obtained from the moving-window GMC/strain softening FEM model.

2. Model development

The model is aimed at capturing the heterogeneity in the material structure and how that heterogeneity translates to material performance. This heterogeneity has two major sources: the random configuration of aggregates within the mortar, and the random strengths of the constituent materials and their interfaces. Random configuration of composites such as concrete can be addressed through stochastic simulation of material properties estimated from moving-window GMC (Tregger, *et al.* 2005); however, the random variations in the strengths are poorly understood. Therefore, the current work is focused on identifying the random interfacial and mortar strengths that are appropriate for application in the moving-window GMC context. In order to isolate the effects of the strength parameters, simple deterministic aggregate geometries are used to reconcile the model with the experiments.

Once the strength parameters are understood, they can be applied in a moving-window GMC context in order to model the effect of overall concrete heterogeneity on its performance. Once the effect of heterogeneity within a given mesostructure can be modeled accurately, then the techniques can be extended using a Monte Carlo simulation to model random heterogeneities that will occur from one mesostructure to the next. In order for the proposed model to improve upon previously existing approaches, it must possess several key attributes. First, the model must be computationally efficient in order to run many simulations. Second, the model must be free of any geometrical assumptions concerning the size, shape and placement of inclusions. Lastly, the model must be able to capture the influence of the local microstructure. A combination of a moving-window Generalized Method of Cells and a Finite Element Method (FEM) approach with a cohesive crack model is adapted in order to satisfy these requirements. Fig. 1 shows the information flow from a digitized mesoscale image to



Fig. 1 Information flow through proposed model

the corresponding deformation and failure behavior. Each step of the process is described in the sections that follow, and more detail can be found in Tregger, *et al.* (2005).

2.1. Image digitization

Image digitization begins with an image of the material structure. In the present study, digital photographs are used, but any imaging technique, such as nano-indentation, SEM petrography, etc., can be used for the desired scale. Once an image is acquired, all the inclusions are identified and the image is filtered into a binary array, in which each material phase is represented by either a 0 or a 1.

2.2. Moving-window micromechanics

Digitized mesostructures could conceptually be applied directly to a finite element model with each pixel being represented by an element in the mesh (e.g. García, *et al.* 2002). Such a model would be extremely costly, however, when trying to assess potential debonding at every finite element interface. An alternative approach is to identify a series of mechanical properties, such as stress-strain curves, that characterize regions within the mesostructure. It is these local mechanical properties that can then serve as input to a subsequent finite element mesh, avoiding the need for explicit debonding in the finite element model.

A schematic of the moving-window approach is shown in Fig. 2, in which 3×3 windows are extracted and analyzed in order to establish a smoother set of local mechanical properties associated with different locations in the mesostructure. In a paper by Graham-Brady, *et al.* (2003) a number of micromechanics models were assessed for relating the local window configuration to related elastic properties, and in that work it was shown that GMC serves as an accurate and computationally efficient basis for the moving-window analyses. A moving-window GMC (MW-GMC) model similar to the method developed by Corr and Graham (2003) is used in this work to capture the local properties of concrete with debonding. In MW-GMC, each window is taken to

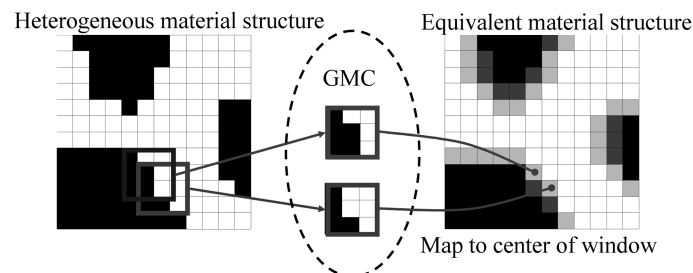


Fig. 2 Moving-window process for sample mesostructure

represent the full GMC periodic cell, and the pixels within the windows are treated as subcells. The results are taken as the effective orthogonal properties of the center subcell. The suite of local results lead to a database that contains the local mechanical properties corresponding to the entire mesostructure. Although a 3×3 moving-window is used for the current model, any suitable size may be used depending on the size of the GMC cell and the distribution of inclusion sizes in the material structure. For further discussion on MW-GMC, see, Corr and Graham (2003).

2.3. Generalized method of cells

Significant literature exists that outlines the generalized method of cells (GMC) (e.g. Paley and Aboudi 1992, Herakovich 1998, Aboudi 1987 and Herakovich and Hidde 1992), but for the purpose of clarification a very brief review is provided here. GMC was originally developed to analyze repeating material structures such as fibrous composites (Paley and Aboudi 1992). In GMC, a material structure, which is represented as a cell, is divided into subcells where each subcell represents a single material type (usually matrix or inclusion). By imposing periodic boundary conditions on the cell boundaries and continuity of average tractions and displacements at the subcell boundaries, the homogenized mechanical properties of the composite are determined. A significant advantage of GMC is that it predicts orthotropic local material properties, which is more consistent than an isotropic assumption within the context of a heterogeneous medium.

Typical implementations of GMC concern both elastic and inelastic materials. In order to account for the quasi-brittleness of concrete the cohesive crack model (Hillerborg, *et al.* 1976) is applied in the GMC formulation, similar to models used by Aboudi (1987) and Herakovich (1992). The basis of this technique is to define tensile stresses at which the interfaces between subcells are activated. Once activated, the interface increases in width, thus adding an additional displacement term to the displacement continuity equations of GMC. Introduction of this displacement discontinuity results in material softening of the concrete. It is important to note that in this analysis the subcells are assumed to remain linear-elastic, so that only the subcell interfaces lead to strain-softening.

The rate of softening is determined by a function which is obtained from experimental or theoretical curves for each interface type (mortar-mortar, aggregate-aggregate, mortar-aggregate). The output from GMC is a full stress-strain curve in the two transverse directions and in shear. These stress-strain curves are then efficiently implemented for each element of the finite-element mesh.

2.4. Strain-softening FEM

An array of local mechanical properties is available from the moving-window GMC that can be analyzed under realistic loading conditions using a strain-softening FEM (SS-FEM) model. Strain-softening is essential to finite element analyses of materials that exhibit quasibrittle cracking and failure behavior; however, it is also a challenge, as negative tangent moduli in the post-peak region can result in non-positive definite stiffness matrices and lead to algorithmic instability. A suitable SS-FEM approach for use with the MW-GMC results is a combination of a secant modulus stiffness (SMS) model outlined by Bhattacharjee and Leger (1993) and a saw-tooth softening model proposed by Rots and Invernizzi (2004). With these models, decreasing secant stiffnesses (as opposed to negative tangent stiffness) represent the degradation of the softening material. A complete description of these methods and how they are implemented with MW-GMC can be found in Tregger, *et al.* (2005), Bhattacharjee and Leger (1993) and Rots and Invernizzi (2004).

2.5. Stochastic modeling

Concrete exhibits random heterogeneities in the configuration of the aggregates within the mortar phase, which can be modeled through Monte Carlo simulation of local mechanical properties. These simulations are based on statistics estimated from the properties of the original image, obtained from moving-window GMC. This has been addressed in papers by Corr and Graham (2003) and Tregger, *et al.* (2005). When considering materials in which the interface dictates critical behavior, however, it is not only the configuration of the mesostructure but also the variations in the interfacial properties and strength that are critical. The issue to be addressed in this work is the random variations in the interfacial properties and in the mortar and aggregate strengths. The strengths of the mortar and aggregate are reflected in the interfacial strengths at the mortar-mortar and aggregate-aggregate subcell interfaces, respectively.

When material mesostructures with random interfacial properties are considered, the mechanical properties for each interface are assigned using Monte Carlo simulation. For the purposes of demonstration in this work, the interfacial strengths are assumed to follow a Gaussian distribution. The technique can be applied easily to simulate strengths coming from any probability density functions, such as the Weibull distribution, without any changes to the general approach.

The current model accounts for two levels of variability: the global strengths that vary from sample to sample, and the local strengths that describe local fluctuations in strength around the random global value. A two-level assignment is used, by which the global tensile strength for each material and interface type are simulated first, and then for each subcell interface the local tensile strength is varied about the random global value. It should be noted that since the mean and variation of the mechanical properties are obtained from experiments, the values will include other sources of uncertainty such as experimental uncertainty.

Simulation of the interfacial strengths is achieved through simple random number generation. On the global level, the interfacial strengths vary randomly from sample to sample, but the mortar-mortar and mortar-aggregate values are correlated such that a high mortar tensile strength will result in a high mortar-aggregate tensile strength. For simplicity, the aggregates are assumed to be infinitely strong and are therefore not assigned a strength value. On the local level, each subcell is assigned a different random number. As such a mortar-mortar bond may be weaker than a mortar-aggregate bond for a particular set of subcells, but on the average this will not be the case. This method of assigning random strengths results in a weakest-link failure, where the peak stress is directly related to the strength of the weakest element.

It is important to realize the difference between the mean of a material property for a specimen and the mean of the “weakest links” for a group of specimens. Fig. 3 shows a group of four

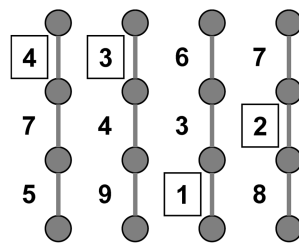


Fig. 3 Mean of the “weakest links” versus mean of the material

different specimens each represented as a chain.

Under tensile stress, each chain will break at its weakest link. The mean of the weakest links therefore is the mean of the boxed numbers, which in this case would be 2.5 $((4+3+1+2)/4)$. On the other hand, the mean of the material for the group would simply be the mean of all the strengths, which is 4.9 $((4+7+5+3+4+9+6+3+1+7+2+8)/16)$. From this simple diagram it can be seen that the mean strength of the weakest links will always be less than or equal to the mean strength of the material.

From experimental results, the mean strength and standard deviation represent the mean strength and standard deviation of the weakest links. However, the current model requires a material mean strength as an input. If the experimental mean and standard deviation are used directly, the model will always under-predict the strength. To rectify the situation, a parametric study will be required after the experimental parameters are acquired.

3. Experimental program

In order to describe the complete tensile stress-strain curve of concrete, three parameters are required: Young’s modulus E , the tensile strength σ_t , and fracture energy G_f . Poisson’s ratio, which affects multi-axial behavior, is considered constant in this study. In GMC, cohesive debonding is possible along every interface: aggregate-matrix, aggregate-aggregate, and matrix-matrix. Cohesive parameters must be measured or estimated for each of these interface types. It is difficult to estimate these properties, as local-area stresses and strains are likely to be highly variable compared to bulk measurable behavior. This section will focus on the cohesive properties of the mortar-mortar and mortar-aggregate interfaces, assuming that the aggregates are significantly stronger than the mortar and the mortar-aggregate interfaces and therefore can be assumed not to fail.

Table 1 Experimental results

	σ_t (MPa)	E (GPa)
Mortar	2.50	25.5
Aggregate	7.00	61.2
Interface	2.11	-

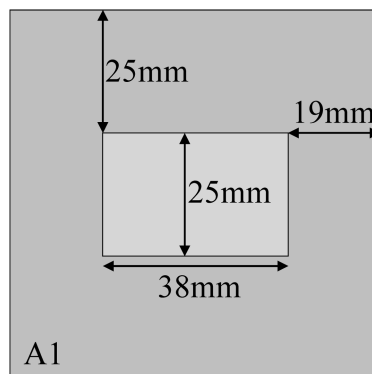


Fig. 4 Single-aggregate specimen schematic

Mechanical properties for the mortar were taken from six direct tensile test results of mortar specimens with water-to-cement ratio, $w/c = 0.485$ and sand-to-cement ratio, $s/c = 2.75$. The mortar was cured in 100% relative humidity for seven days before being tested. The free area of the prism specimen is 76×76 mm, and the specimens are 25 mm thick. The specimen is loaded in a displacement controlled closed loop testing system, with the average of two LVDT displacements (from each side of the prism) as the feedback, with a rate of 0.0025 mm/min. The resulting mean strength and elastic modulus values from these tests are given in Table 1. Stress-displacement curves are extracted from these tests, and serve as an estimate for the strain softening behavior.

For the mortar-aggregate properties, a single-aggregate specimen is used to estimate the behavior of the interface. A schematic of the single-aggregate specimen used to extract the mortar-aggregate interface bond strength is shown in Fig. 4.

The visible cross section of the granite is constant through the thickness, and is thus referred to as a two-dimensional “model concrete” specimen (Gopalaratnam and Shah 1985). The experiment is designed so that a relatively even level of stress is applied to the aggregate-mortar interface. Table 1 contains the material properties taken from the experiments. The shape parameters in the GMC model can be calibrated from the experimental results so that for a given specimen size and tensile strength, the resulting stress-displacement curve will match that of the experiments.

4. Parametric study

A parametric study is carried out in order to account for the weakest link principle, described above. In the parametric study, the local coefficients of variation of the tensile strengths and the input tensile strengths for the mortar and interface are varied since these are the factors that influence the mean of the bulk tensile strength. Two studies are done; the first study varies the local coefficient of variation of the tensile strength while holding the input tensile strengths constant, and the second study varies both input tensile strengths (keeping the ratio between the two constant) and keeping the coefficient of variation constant. Both of these studies apply to the single-aggregate model.

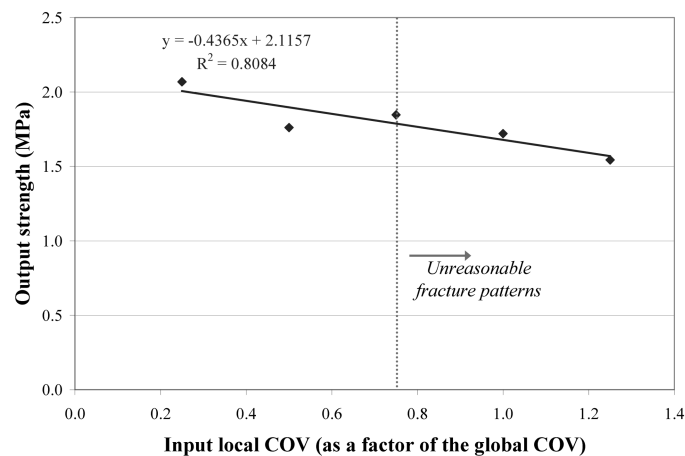


Fig. 5 Effect of local uncertainty on model mean and variation of bulk strength

The first study varies the coefficient of variation from 0.25 times the global coefficient of variation of the single-aggregate experimental results (16.9%) to 1.25 times the global coefficient of variation. The input interface strength is taken as 2.11 MPa and the input mortar strength is taken as 2.50 MPa. Fig. 5 shows the influence of the coefficient of variation on the mean and variation of the bulk strength.

From Fig. 5, there is a dependence between the local uncertainty and the bulk output strength; as the local uncertainty increases, the bulk strength decreases. This is intuitive since the wider the local variation is, the lower the strength will be of the weakest element. The bulk variation in the tensile strength is correlated to the local variation as shown by the R^2 value. The dotted line in Fig. 6 represents a boundary between reasonable and unreasonable results concerning fracture propagation in the specimens. Beyond the dotted line, fracture paths become excessively discontinuous, which is not characteristic of the experimental results. Fig. 6 shows an example of a discontinuous fracture path.

The rectangle shows the approximate location of the aggregate. The model reaches the axial strain limit of the program since there exists a set of cracks that stretch from one side to the other. Because this behavior was not seen in the experiments, the local variation is limited to 0.50 times

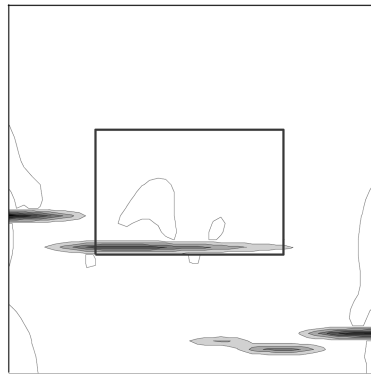


Fig. 6 Axial strain contour plot showing discontinuous fracture path from model with excessive local variation

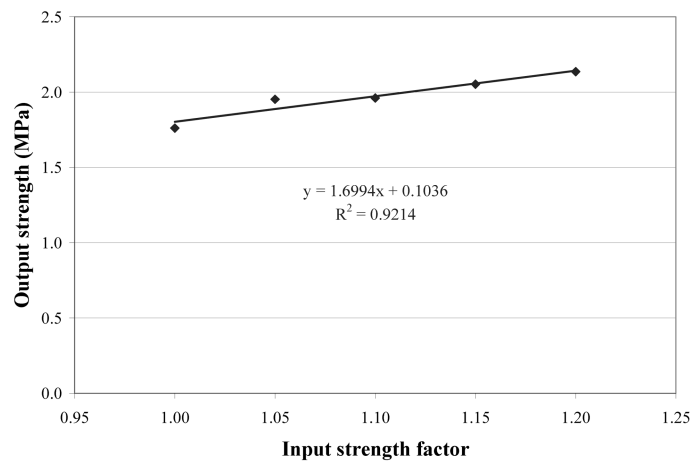


Fig. 7 Effect of tensile strength on model mean and variation of bulk strength

Table 2 Calibrated material parameters for model input

	σ_i (MPa)	E (GPa)
Mortar	2.75	25.5
Aggregate	7.00	61.2
Interface	2.32	-

the global coefficient of variation. The actual factor used for all the specimens is 0.30; that is the local variation is 0.30 times the global variation for a particular specimen type. The global variation is extracted from the experimental data.

The next study shows the effect of input tensile strength on the bulk strength of the specimen. The tensile strengths of both the mortar and interface were varied by factors of 1.0 to 1.2. A local coefficient factor of 0.50 is assumed and held constant. Fig. 7 shows the results of the second study.

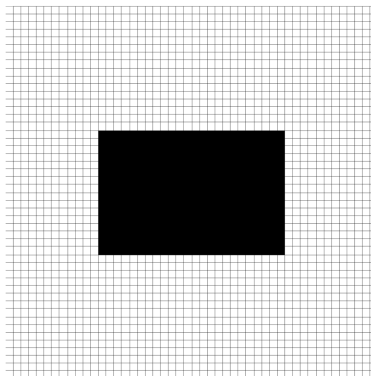
Fig. 7 shows that as the input tensile strengths are increased, the mean bulk strength increases as well, which is expected. The input strengths are strongly correlated to the coefficient of variation of the tensile strengths as shown by the high R^2 value. The multiplication factor used for all the specimens is 1.10. Note that this value will give an output strength lower than the desired 2.1, but because the local coefficient factor is 0.30 and not 0.50, the adjustment of the input strength factor should be less. From these two parametric results, more realistic input values can be selected to counter the effect of the weakest link principle, as shown in Table 2.

5. Analysis results and discussion

5.1. Single-aggregate specimen

A 48×48 pixel mesh shown in Fig. 9 is analyzed to confirm the results of the parametric study. Each pixel in Fig. 8 represents a 1.58 mm square. The right and left edges are traction free while the load is applied to the top edge. The bottom edge is considered fixed.

A typical contour map of the tensile strengths in the y-direction is shown in Fig. 9. The weakest zones lie along the interfaces, but weak zones also exist in the mortar. The mechanical properties representing thirty simulations are shown in Table 3 and are compared with the results from the experiments.

Fig. 8 48×48 mesostructure for A1 specimen

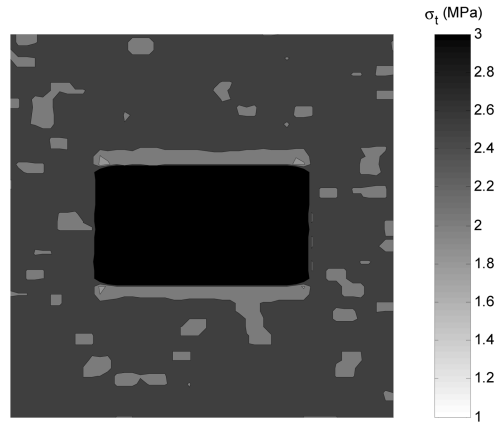


Fig. 9 Tensile strength contour map for A1 specimen

Table 3 Comparison of mechanical properties between experiments and model for A1 specimen

Experiment	σ_t (MPa)	E (GPa)
μ	2.11	28.1
δ (%)	16.9	7.5
Model	σ_t (MPa)	E (GPa)
μ	2.07	27.2
δ (%)	14.1	
% Error	σ_t (MPa)	E (GPa)
μ	1.8	3.3
δ (%)	18.0	

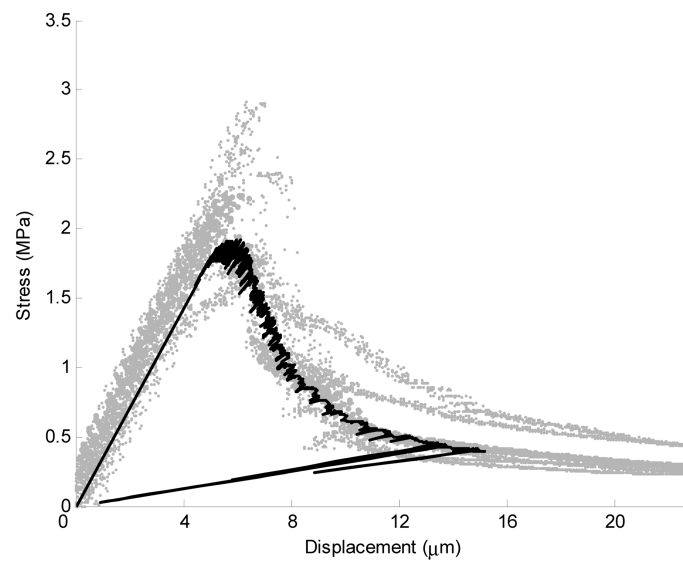


Fig. 10 Typical stress-displacement curve for A1 model specimen

The mean strength and elastic modulus of the model agrees with the experimental data. However, the model exhibits somewhat less variation than the experiments. This could be due to a number of reasons, including the fact that the model only incorporates material uncertainty, while the experiments add other variations: human factors, alignment, etc. A typical stress-displacement curve is plotted against several representative experimental results in Fig. 10. The model is able to represent the post-peak behavior as well as peak strengths.

Fracture for these simulations usually occurs at either the top or bottom of the aggregate. The fracture progression for the models is similar to the experiments: the crack initiates at the mortar-aggregate interface and propagates towards the edges through the mortar. The A1 specimen analysis confirms the model's ability to match the experimental data after adjusting the input parameters to correct for weakest link.

5.2. Three-aggregate specimen

To examine the model framework's ability to predict behavior of different material arrangements, the A3a specimens, shown as a 48×48 pixel mesh shown in Fig. 11, are analyzed.

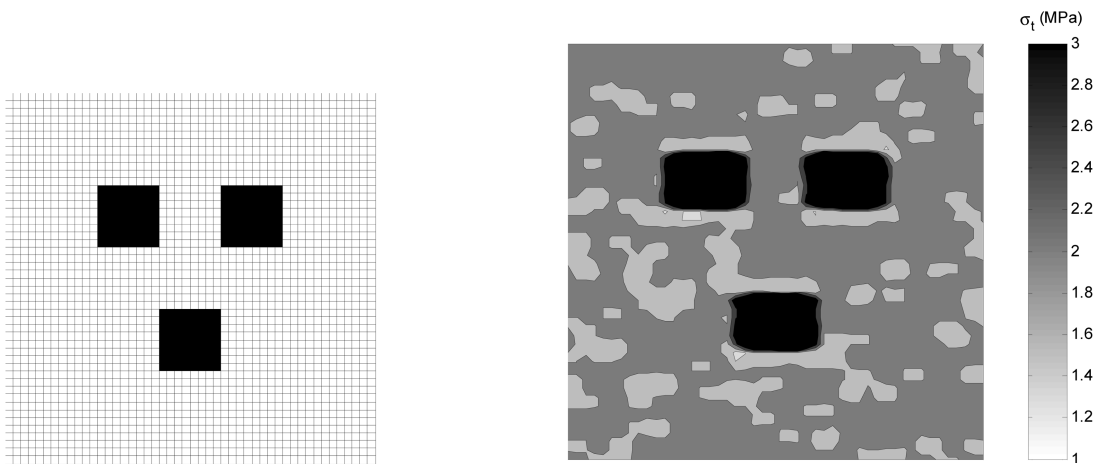


Fig. 11 48×48 mesostructure for A3a specimen Fig. 12 Typical tensile strength contour map for the A3a specimen

Table 4 Comparison of mechanical properties between experiments and model for A3a specimen

Experiment (25)	σ_t (MPa)	E (GPa)
μ	1.77	25.4
δ (%)	35.4	17.0
Model (30)	σ_t (MPa)	E (GPa)
μ	1.84	25.5
δ (%)	36.6	
% Error	σ_t (MPa)	E (GPa)
μ	-4.1	-0.2
δ (%)	-3.2	

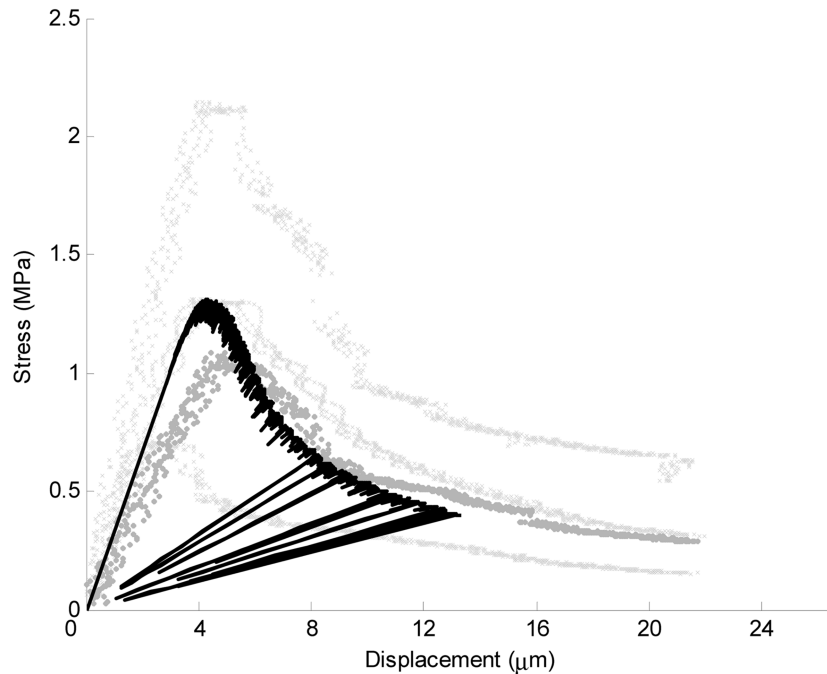


Fig. 13 Typical model stress-displacement curve for the A3a specimen (Soil line represents model, dots represent experimental data).

Table 5 Comparison of tensile strength based on fracture location for A3a specimen

Fracture location	Experiment	Model	% Difference
Inside	1.91	2.05	7.05
Outside	1.59	1.58	0.99

A typical contour map of the tensile strengths in the y-direction is shown in Fig. 12. Again, the weakest zones correspond to the interfaces, but weak zones also exist in the mortar.

The mechanical properties representing thirty simulations with their comparisons to the experiments are shown in Table 4 while Fig. 13 shows a typical stress-displacement curve plotted against representative experimental data.

Of a total of thirty specimens, eighteen specimens fractured inside the aggregate arrangement (62%) while eleven fractured outside of the aggregate arrangement (38%). These numbers are comparable to the experimental results (65% inside the aggregate arrangement and 35% outside the aggregate arrangement.). The remaining fracture occurs strictly through the mortar near the steel plates. A summary of these fracture locations is given in Table 5.

The model shows good agreement with the mechanical properties and their statistics of the experiments, namely that the inside region is stronger than the outside region. Also, fracture behaviors are reproduced. When comparing the two different pre-arranged aggregate specimens, the single-aggregate specimen has a higher strength than the triple-aggregate specimen. This can be attributed to a weakest-link type phenomenon. The single-aggregate specimen will achieve a certain high strength when the mortar-aggregate interface is strong enough. However, for the triple-

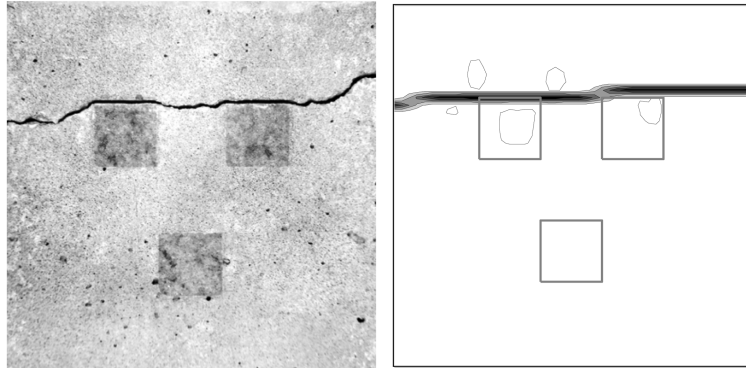


Fig. 14 Similar fractures outside the aggregate arrangement for experiment and model

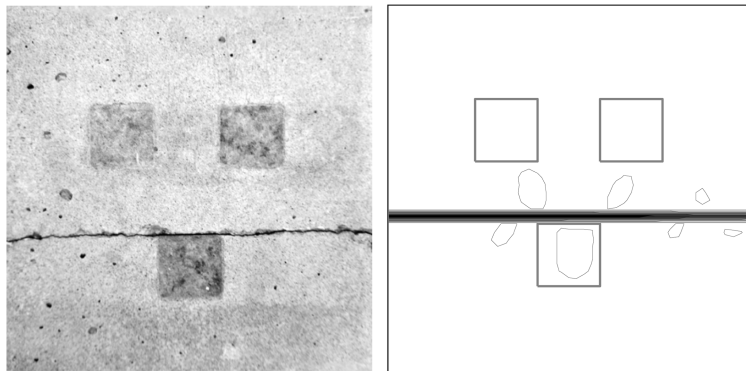


Fig. 15 Similar fractures inside the aggregate arrangement for experiment and model

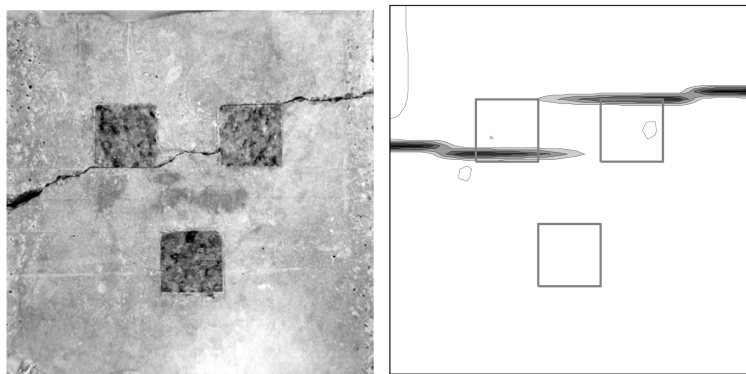


Fig. 16 Similar non-standard fractures for experiment and model

aggregate specimen to achieve the same high strength, all mortar-aggregate interfaces must be strong enough. The probability of this happening is much lower than for the single-aggregate, and the result is the lower strength seen for these specimens.

6. Future work

The real value of the proposed model lies within its ability to model spatially varying material structures. Future work will include incorporation of the random mortar strength and random mortar-aggregate interfacial properties into moving-window GMC models of concrete with random mesostructure. Such models could be reconciled with Bolander's work (1998), which implemented discretized models based on Voronoi diagrams. It will also be critical that the model be extended to three-dimensional analysis, in order to best represent the true nature of concrete behavior. Such three-dimensional mesostructures can be obtained from x-ray microtomography or serial sectioning techniques. Other areas of future work include the ability to randomize the modulus and fracture energy in addition to the tensile strength. Correlation of these variables is also recommended; for example, areas of low tensile strength are likely to also have low elastic moduli. In addition, although this study considers debonding at the aggregate interface, other mechanisms such as aggregate interlocking are important, and should be investigated in the future.

7. Conclusions

The following general conclusions can be made from this work:

- For mesoscale analysis, assuming mortar-aggregate interface properties such as tensile strength from single-aggregate experiments is acceptable; however, adjustments must be made due to the "weakest link" effect.
- In pre-arranged aggregate specimens, tensile strength and modulus correlate with fracture locations.
- The proposed model can capture basic behavior of pre-arranged aggregates in regards to the mean and variation of strength as well as fracture path.

References

- Aboudi, J. (1987), "Damage in composites – modeling of imperfect bonding", *Compos. Sci. Technol.*, **28**(1), 103-128.
- Baxter, S. C., Hossain, M. I., and Graham, L. L. (2001), "Micromechanics based random material property fields for particulate reinforced composites", *Int. J. Solids Struct.*, **30**, 9209-9220.
- Bazant, Z. P. and Oh, B. H. (1983), "Crack band theory for fracture of concrete", *Mater. Struct.*, **16**(93), 165-205.
- Bazant, Z. P. and Yu, Q. (2003), "Reliability, brittleness and fringe formulas in concrete design codes", *Infrastructure Technology Institute*, 03-12/A475.
- Bentz, D. P. (April 2000), "CEMHYD3D: A three-dimensional cement hydration and microstructure development modelling package", Version 2.0. NISTIR 6485, US Department of Commerce, Available from: <<http://www.bfrl.nist.gov/861/vcctl/>>.
- Bhattacharjee, S. S. and Leger P. (1993), "Finite element modeling of the tensile strain softening behaviour of plain concrete structures", *Eng. Comput.*, **10**(3), 205-221.
- Bolander, J. E. and Saito, S. (1998), "Fracture analysis using spring networks with random geometry", *Eng. Fract. Mech.*, **61**(5-6), 569-591.
- Corr, D. J. and Graham, L. L. (2003), "Mechanical analysis of concrete with the moving-window generalized method of cells", *ACI Mater. J.*, **100**(2), 156-164.
- Choi, S. and Shah, S. P. (1999), "Propagation of microcracks in concrete studied with subregion scanning

- computer vision (SSCV)", *ACI Mater. J.*, **96**(2), 255-260.
- García, R. E., Langer, S. A. and Carter, W. C. (2002), "Finite element implementation of a thermodynamic description of piezoelectric microstructures", *J. Am. Ceram. Soc.*, **49**(5), 395-407.
- Gopalaratnam, V. S. and Shah, S. P. (1985), "Softening response of plain concrete in direct tension", *ACI J.*, **82**(3), 310-323.
- Graham-Brady, L. L., Siragy, E. F. and Baxter, S. C. (2003), "Analysis of heterogeneous composite materials using moving-window techniques", *J. Eng. Mech.*, **129**(9), 1054-1064.
- Graham-Brady, L. and Xu, X. F. (2007), "Stochastic morphological modeling of random multiphase materials", *ASME J. Appl. Mech.*, in press.
- Grigoriu, M., Garboczi, E. J. and Kafali, C. (2007), "Spherical harmonic-based random fields for aggregates used in concrete", *Powder Tech.*, **166**(3), 123-138.
- Herakovich, C. T. (1998), *Mechanics of Fibrous Composites*, John Wiley & Sons, Inc., New York, NY.
- Herakovich, C. T. and Hidde J. S. (1992), "Response of metal matrix composites with imperfect bonding", *Ultramicroscopy*, **40**(3), 215-228.
- Hillerborg, A., Modéer, M. and Petersson, P. E. (1976), "Analysis of crack formation and crack growth in concrete by means of fracture mechanics and finite elements", *Cement Concrete Res.*, **6**(6), 773-782.
- Landis, E. N., Nagy, E. N., and Keane, D. T. (2003), "Microstructure and fracture in three dimensions", *Eng. Fract. Mech.*, **70**(7), 911-925.
- Paley, M. and Aboudi, J. (1992), "Micromechanical analysis of composites by the generalized cell model", *Mech. Mater.*, **14**, 127-139.
- Rots, J. G. and Invernizzi, S. (2004), "Regularized sequentially linear saw-tooth softening model", *Int. J. Numer. Anal. Methods Geomech.*, **28**(7-8), 821-856.
- Sutton, M. A., McNeill, S. R., Helm, J. D. and Schreier, H. W. (2000), "Computer vision applied to shape and deformation measurement", In: Rastogi PK, Inaudi D, eds. *Trends in Optical Nondestructive Testing and Inspection*, Elsevier Science B. V., 571-589.
- Tregger, N. A., Corr, D. J., Graham-Brady, L. L. and Shah, S. P. (2006), "Modeling the effect of mesoscale randomness on concrete fracture", *Prob. Eng. Mech.*, **21**(3), 217-225.